

INITIAL VERIFICATION OF A 3D MORPHOGENETIC MODEL OF IN-FLIGHT ICING ON A CYLINDER

Krzysztof Szilder*, Edward P. Lozowski**

*Institute for Aerospace Research, National Research Council, Ottawa, Canada

** University of Alberta, Edmonton, Canada

Abstract

In this paper, we verify the results of a three-dimensional morphogenetic model simulating rime and glaze ice accretion structures forming on a circular cylinder. Using a novel approach, we predict the shape and structural details of aircraft ice accretions by emulating the behaviour of individual fluid elements. In the model, the airflow and droplet trajectories are confined to planes perpendicular to the axis of a cylinder, but the resulting ice accretion is, nonetheless, fully three-dimensional. The model predicts rime, glaze and simultaneous glaze and rime accretions. A partial verification of the model has been accomplished and although there are discrepancies between experimental and predicted accretion shapes, the overall agreement is good. In particular, the prediction of the stagnation line growth rate agrees well with experimental data. This satisfactory verification suggests that morphogenetic modeling is a viable alternative for the simulation of in-flight icing. Practical implementation of this approach will require coupling the model to an external flow field solver as well as to heat transfer and droplet impingement solvers.

1 Introduction

Wind tunnel experiments and in-flight observations show that the form of aircraft ice accretions is often rough, highly convoluted and discontinuous, with evident three-dimensional features. Natural ice accretions also tend to be difficult to reproduce, in the sense that no two ice accretions are identical, even when grown

under essentially identical conditions. Variations of the ice accretion shape and structure are experimentally observed along cylinder and airfoil surfaces exposed to uniform atmospheric conditions. Nevertheless, most current icing models predict accretion shapes that are relatively smooth and coherent because they are based on the solution of continuous equations [1-4]. Moreover, most existing models are also perfectly reproducible in the sense that two identical sets of input conditions will lead to two identical results, at least for a single model. In this sense, most existing models are inherently unable to reproduce some of the fundamental aspects of in-flight ice accretion. Exceptions are the so-called “morphogenetic models”, originally conceived by Szilder [5] and applied recently to in-flight icing [6 and 7].

The morphogenetic model used here is a cellular automaton that emulates the motion and freezing of discrete fluid elements on the accretion surface. The domain is a three-dimensional cubic lattice. The model fluid elements are cubes with sides that are a fraction of millimetre. Each fluid element begins a random walk from its initial stochastic impact location, moving downstream along the surface. At each step in the process, a random draw determines whether an element freezes or continues to move along the ice surface. There is only one unfrozen element on the surface at a time. The model is intrinsically stochastic, although the results are reproducible if a known sequence of pseudo-random numbers is used. No two realizations with different random number sequences are identical, although bulk

parameters such as mass and shape are typically very similar. This stochastic capability is unique to the present model. It reflects the fact that, under natural icing conditions, we do not know the behaviour of individual cloud droplets. Yet, collectively, this individual behaviour can lead to variations from one case to another.

This paper describes initial verification of a 3D version of the model for icing on a cylinder under in-flight conditions. In two recent papers [6 and 7], we modelled the shape and structure of 2D ice accretions forming on a circular cylinder. However, because the model's strength is its ability to simulate discrete structures, we have moved quickly to formulate a 3D version. In [8], we examined the formation of "lobster tails" or "scallops" forming on swept wings. However, our analysis of the results in that paper was qualitative and we could not make claims concerning the quantitative accuracy of the model. In addition, the lobster tail model was restricted to cases with little or no runback. Our objective in this paper is to show that the morphogenetic model can be used to predict three-dimensional rime and glaze accretions with runback. In order to compare with our experimental results, we simulate ice formation on a circular cylinder.

2 Three-Dimensional Ice Accretion Model

Our two-dimensional morphogenetic model has already been described fully in [6 and 7]. Consequently, we will describe here only the main features of the 3D model and the modifications that were made to introduce three-dimensionality. For mathematical formulations and model details the reader should refer to the previous papers.

Morphogenetic models consist of a particle trajectory model that determines the impact location of individual fluid elements, and a random walk model, that emulates their behaviour on the cylinder or ice surface. A heat transfer model is also used to determine the probability of freezing of the elements. Because of computing limitations, the model fluid

elements are typically larger than individual cloud droplets. Consequently, we like to think of them as ensembles of cloud droplets, all of which undergo identical histories. A three-dimensional cubic lattice defines the accretion domain. By building the ice accretion one particle at a time, a morphogenetic model simulates the time evolution of the accretion shape in a natural way.

In the model, a circular cylinder is placed perpendicular to an initially uniform airflow and exposed to impinging supercooled droplets. The streamlines and droplet trajectories lie in a vertical plane perpendicular to the cylinder axis. However, the model exists in a fully three-dimensional space. The fluid elements impact randomly on the cylinder surface or on the existing ice structure, in such a way that the impacting mass distribution is consistent with the collision efficiency distribution computed for a single droplet size on a clean cylinder. There is no recomputation of the collision efficiency distribution once ice has begun to accrete. As soon as a particular fluid element freezes or leaves the domain, the next element is released. The total number of released fluid elements is determined by the total inbound water mass, which is the product of free-stream velocity, liquid water content and duration of the icing event.

In the glaze region, where there is surface liquid flow (runback), the fluid elements move downstream. Once a particle has moved to an adjacent cell, a pseudo-random number, between zero and unity, is generated. If this number is less than the local probability of freezing, the particle freezes, otherwise it moves on. The method to calculate the local probability of freezing from the heat transfer distribution is derived in [7]. When a fluid element freezes, it does not necessarily remain in the cell where freezing occurs. Instead, a cradle location is sought in the neighbourhood of the freezing grid cell. Since the model is three-dimensional, this neighbourhood is defined by a sphere, centred on the initial freezing cell, with a radius, expressed in grid cell lengths, of 3. The freezing fluid element is moved to an empty cell within

this sphere where it has the largest number of occupied neighbours (consisting of cylinder surface cells or already frozen particles). If there is more than one such location, the final site is chosen randomly from among them.

In the rime region, where there is no runback, fluid elements freeze on impact, but a cradle location is still sought out within one grid cell radius. The three-dimensionality of the model is taken into account by establishing a new relation between atmospheric conditions and ice density using experimental data. For details of the method, as applied in 2D, the reader is referred to [7].

3 Model Results and Discussion

In order to compare with previous experimental results [9], we examine the ice accretion on a circular cylinder, 2.54 cm in diameter, produced by monodisperse supercooled droplets of 20 μm diameter. Ranges of airspeed and static temperature were run in the icing wind tunnel experiments, and these have been reproduced in the model. Morphogenetic model simulations were performed on a three-dimensional cubic lattice consisting of 150 by 150 by 100 (along the cylinder axis) cells, with a cell dimension of 0.25 mm. The fluid elements are cubes, each occupying one grid cell (0.015625 mm^3) after freezing. All computations were performed on one node of a Linux cluster with dual Pentium 4 Xeon 2.2 GHz CPUs, 512KB L2 cache and 2GB RAM. For this domain, the simulation time varies between about 15 and 60 minutes, depending on the total number of fluid elements and the atmospheric conditions. In 60 minutes of CPU time, it is possible to track about 300,000 fluid elements, one at a time.

Figures 1 and 2 compare model and experimental accretion shapes, the latter produced in the Altitude Icing Wind Tunnel at NRC. The nominal liquid water content was 0.4 gm^{-3} and the static temperatures were -15°C and -5°C , respectively. Model-predicted three-dimensional results are shown next to corresponding two-dimensional experimental

shapes, obtained using a plasticene mold. A 15 mm thick span-wise segment of simulated ice accretion is displayed, looking along the cylinder surface at an angle of 10 degrees from the cylinder axis. This low viewing angle was chosen to facilitate comparison with the experimental cross-sections. Only the surface of the simulated ice shape is shown in green and dark green. The cylinder surface is depicted in black.

When the airspeed is 30.5 ms^{-1} , the model predicts that the entire ice accretion consists of rime ice, Fig. 1a. The roughness of the model ice surface can be easily seen, as can voids, which extend to the cylinder surface, whose prevalence increases with distance from the stagnation line. We conclude that, in the model, hard rime prevails near the stagnation line, while a more porous ice structure exists away from the stagnation line. This porous ice structure occurs near the edges of the ice accretion where rime feathers are observed to grow in the experiments. As yet, however, the model seems unable to reproduce individual rime feathers. At least qualitatively, the model also exhibits various stochastic features of the ice accretion such as roughness, porosity and a lack of symmetry about the cylinder's horizontal plane of symmetry and along the cylinder's axis. This stochastic variability of the model's simulation is due to its fundamental randomness. However, because we have not yet devised a means to quantify these variables in experimental ice accretions, it is not possible to make a quantitative comparison at present. A comparison of the ice growth rate at the stagnation line, measured experimentally and predicted by the model, is shown in Fig. 3. Maximum and minimum values of the model ice growth rate along the stagnation line, $7.5 \mu\text{ms}^{-1}$ and $9.1 \mu\text{ms}^{-1}$, are shown, whereas only a single experimental value is available, $9.1 \mu\text{ms}^{-1}$. An increase in airspeed to 61.0 ms^{-1} , Fig. 1b, leads to an increase of the impingement area, as observed experimentally and predicted by the model. As in the 30.5 ms^{-1} case, the porosity of the rime increases away from the stagnation line. The agreement between the

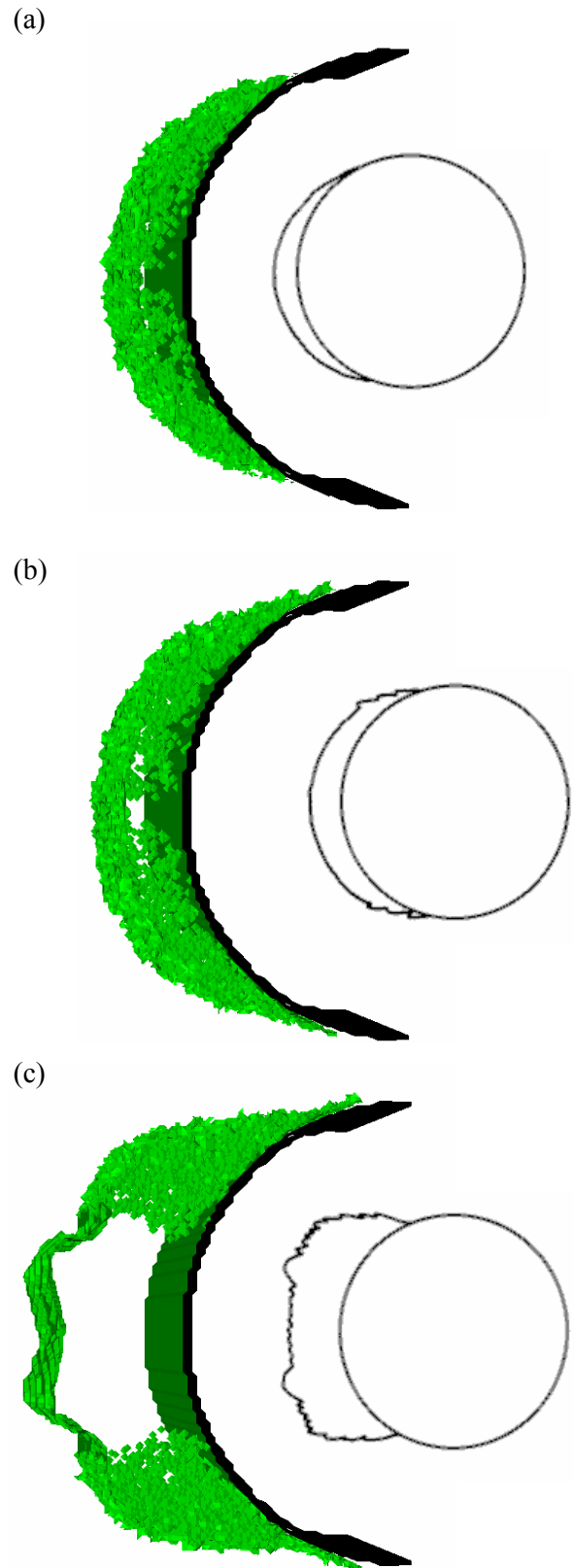
predicted and experimental rime ice shapes and the stagnation line growth rates, Fig 3, is acceptable.

When the airspeed is 122.0 ms^{-1} , Fig. 1c, both the model simulation and the experiment exhibit glaze near the stagnation line with rime further downstream. Water flows away from the stagnation line region, leading to the formation of horns in the high heat transfer zone. In the model, rime ice characterized by a porous accretion forms downstream from the horns. This is generally in the area of experimentally observed rime feathers. The model-predicted surface changes from a comparatively smooth glaze surface to a rough rime ice surface at the transition point. In comparison with the experiments, the model predicts more pronounced horn growth, with a rapidly diminishing rime ice thickness beyond the horns. The differences between the model and experimental ice shapes may be due, in part, to the lack of recalculation of the airflow, collision efficiency and heat transfer during this substantial ice growth. Nevertheless, there is encouraging agreement in the stagnation line growth rates, Fig. 3.

As the static temperature is raised to -5°C , the extent of glaze ice increases. At an airspeed of 30.5 ms^{-1} , regions of glaze and rime coexist, Fig. 2a. The model predicts a glaze region close to the stagnation line, characterized by high density and a comparatively smooth surface. Away from the stagnation line, rime forms with a rougher surface and lower density. The overall agreement between the model predictions and the experiments continues to be encouraging, (see also Fig. 3).

Fig. 1. Model-simulated and experimental accretion shapes for -15°C static temperature and other conditions corresponding to the experiments of Lozowski et al. (1983)^[9].

- (a) Airspeed 30.5 ms^{-1} , liquid water content 0.40 gm^{-3} , icing duration 5.0 min.
- (b) Airspeed 61.0 ms^{-1} , liquid water content 0.46 gm^{-3} , icing duration 2.5 min.
- (c) Airspeed 122.0 ms^{-1} , liquid water content 0.44 gm^{-3} , icing duration 2.5 min.

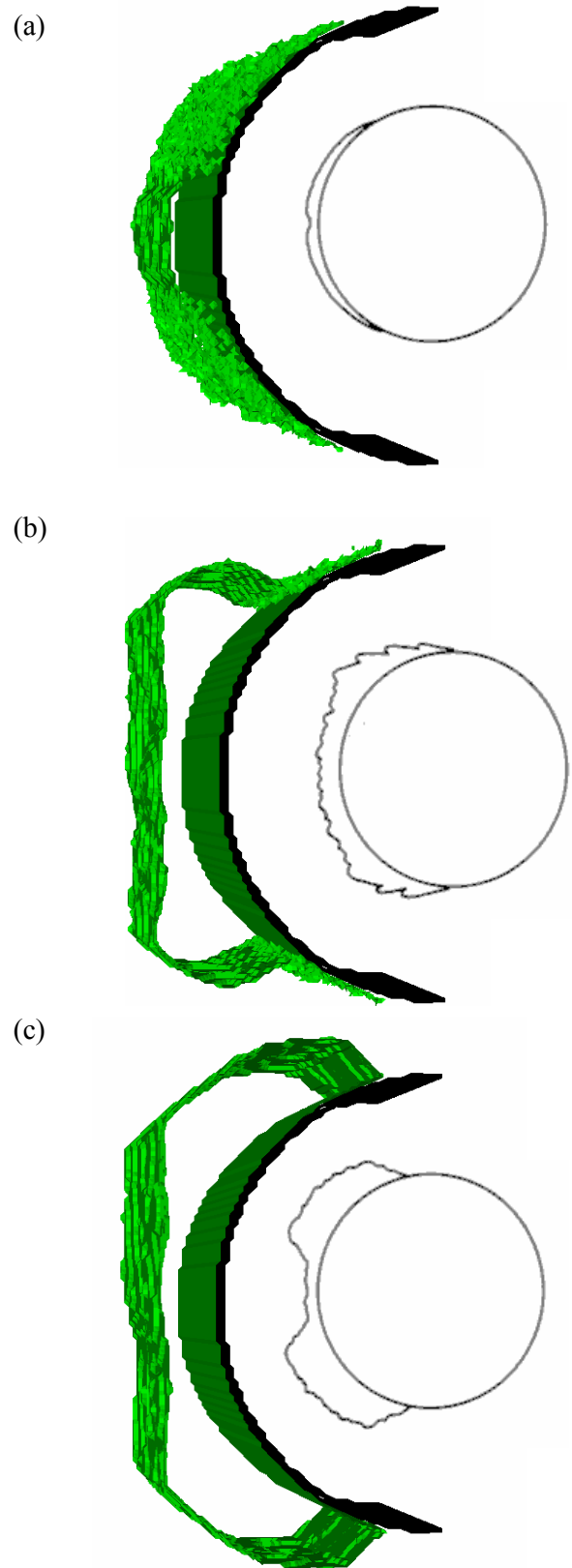


At an airspeed of 61.0 ms^{-1} , Fig. 2b, both model and experiments exhibit similar horns and a glaze/rime transition further downstream. Finally, at an airspeed of 91.5 ms^{-1} Fig. 2c, the model profile is somewhat thicker than the experimental one at the stagnation line, Fig 3.

A comparison between the model-predicted and experimental stagnation line growth rates is shown in Fig. 3. All the experimental results, for static temperatures of -15°C and -5°C , are plotted versus the model maximum and minimum values (along the stagnation line) for the same conditions. In addition to cases already discussed in Figs. 1 and 2, the results are shown for the remaining experiments with nominal liquid water contents of 0.8 and 1.2 gm^{-3} [9]. Overall, there is exceptionally good agreement between the two ice growth rates, although the model does have a small bias towards overprediction. The discrepancy could be due, in part, to an incorrect distribution of the parameterized convective heat transfer coefficient, which does not account for the possibility that the horns themselves may alter the local heat transfer at the stagnation line. Another possible source of differences between the model and experiments is the use of a monodisperse droplet size distribution in the model, with diameter equal to the volume median diameter of the experimental droplet size distribution.

Fig. 2. Model-simulated and experimental accretion shapes for -5°C static temperature and other conditions corresponding to the experiments of Lozowski et al. (1983)^[9].

- (a) Airspeed 30.5 ms^{-1} , liquid water content 0.40 gm^{-3} , icing duration 5.0 min.
- (b) Airspeed 61.0 ms^{-1} , liquid water content 0.46 gm^{-3} , icing duration 4.0 min.
- (c) Airspeed 91.5 ms^{-1} , liquid water content 0.38 gm^{-3} , icing duration 4.0 min.



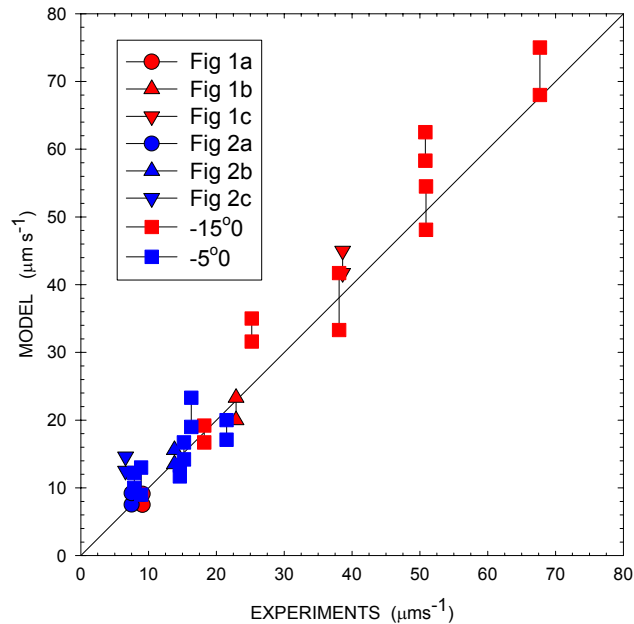


Fig. 3. Comparison of experimental and model stagnation line growth rate [9].

Finally, the model has been used to analyze the influence of air temperature on the ice structure and the location of the horns. At an air temperature of -25°C , the accretion consists entirely of rime ice, Fig. 4a. As a result of decreasing droplet impact speed and decreasing ice surface temperature with increasing azimuthal angle, the rime ice density decreases and surface porosity increases with the azimuth. With increasing static temperature, changes in the model-simulated ice shape may be seen in Figs. 1a and 2a. Yet further temperature increases in the model lead to expansion of the glaze region, the formation of glaze horns, which move downstream with increasing temperature, and the entire disappearance of the rime ice region, Fig. 4b-d.

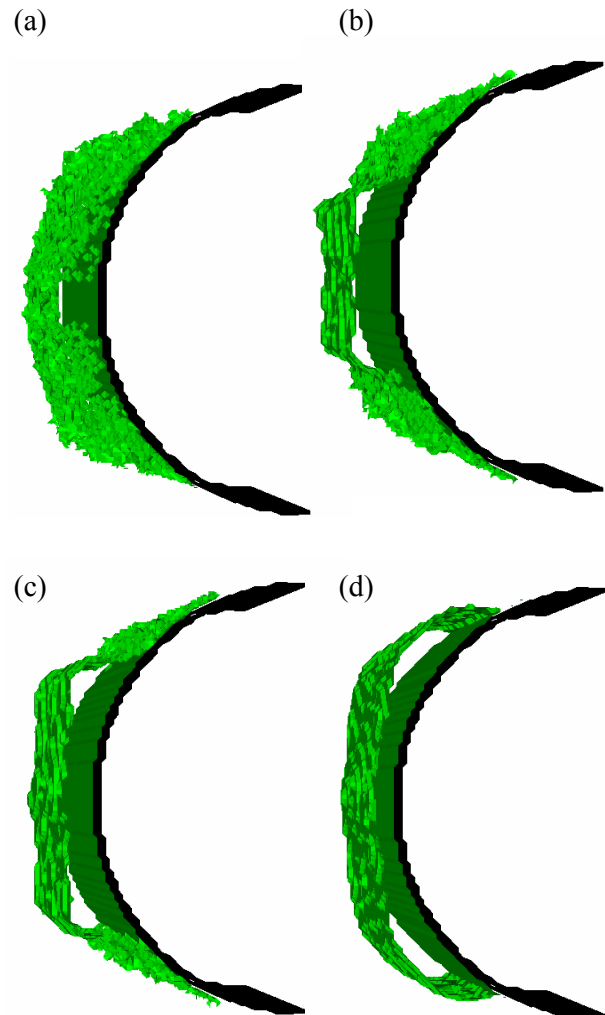


Fig. 4. Model-predicted accretion shape for an airspeed of 30.5 ms^{-1} , liquid water content of 0.40 gm^{-3} and icing duration of 5.0 min.

- (a) Static temperature -25°C
- (b) Static temperature -4°C
- (c) Static temperature -3°C
- (d) Static temperature -2°C

4 Conclusions

A three-dimensional morphogenetic model, for in-flight icing on a circular cylinder, has been described. The model predicts the 3D ice accretion shape, structural details and density over a wide range of atmospheric and flight conditions. Model simulations have been run under rime, glaze and mixed glaze/rime conditions, as a function of the controlling parameters: static temperature, liquid water content, and airspeed. We have performed an initial verification of the model, using comparable icing wind tunnel data. The results are encouraging, indicating that the morphogenetic model can simulate 3D ice accretions on a cylinder, in reasonable agreement with experimental data. Although our model predicts stochastic variability of ice accretion along cylinder surface, we have so far been unable to compare this variation with the experimental variability.

Future work will include using the three-dimensional model to simulate the time-dependent formation of ice accretion on cylinders and airfoils, by recalculating the airflow, droplet trajectories, and the distribution of the convective heat transfer coefficient, as the ice accretion evolves with time. This will require coupling the model to airflow and droplet trajectory models. We also plan to compare model variability with natural variability, which will require devising techniques to quantify the observed experimental variability.

References

- [1] Hedde T and Guffond D. ONERA Three-Dimensional Icing Model. *AIAA Journal*, Vol. 33, No. 6, pp. 1038-1045, 1995.
- [2] Wright W B. Users Manual for the Improved NASA Lewis Ice Accretion Code LEWICE 1.6. *NASA CR-198355*, 1995.
- [3] Morency F, Tezok F and Paraschivoiu I. Heat and Mass Transfer in the Case of Anti-Icing System Simulation. *Journal of Aircraft*, Vol. 37, No. 2, pp. 245-252, 2000.
- [4] Bourgault Y, Beaugendre H and Habashi W G. Development of a Shallow-Water Icing Model in FENSAP-ICE. *Journal of Aircraft*, Vol. 37, No. 4, pp. 640-646, 2000.
- [5] Szilder K. Simulation of Ice Accretion on a Cylinder due to Freezing Rain. *Journal of Glaciology*, Vol. 40, No. 136, pp. 586-594, 1994.
- [6] Szilder K and Lozowski E P. A New Discrete Approach Applied to Modelling of In-Flight Icing. *Canadian Aeronautics and Space Journal*, Vol. 48, No. 3, pp. 181-193, 2002.
- [7] Szilder K and Lozowski E P. Novel Two-Dimensional Modeling Approach for Aircraft Icing. *Journal of Aircraft*, Vol. 41, 2004 (in press).
- [8] Szilder K and Lozowski E P. 2.5-D Modelling of Rime Ice Accretion on a Swept Airfoil. *12th Annual Conference of CFD Society of Canada*, Ottawa, Canada, pp. 495-500, 2004.
- [9] Lozowski E P, Stallabrass J R and Hearty P F. The Icing of an Unheated, Nonrotating Cylinder. Part II: Icing Wind Tunnel Experiments. *Journal of Climate and Applied Meteorology*, 12, pp. 2063-2074, 1983.